CIRP Annals - Manufacturing Technology 71 (2022) 317–320

Contents lists available at ScienceDirect

CIRP Annals - Manufacturing Technology

journal homepage: https://www.editorialmanager.com/CIRP/default.aspx

Real-time estimation of cutting forces via physics-inspired data-driven model

Gregory W. Vogl[a,1,*], Dominique A. Regli[b], Gregory M. Corson[c]

[a] Engineering Laboratory, National Institute of Standards and Technology (NIST), 100 Bureau Drive, Gaithersburg, MD 20899-8220, USA
[b] Department of Mechanical Engineering, Johns Hopkins University, Baltimore, MD 21218, USA
[c] Department of Mechanical, Aerospace, and Biomedical Engineering, University of Tennessee, Knoxville, TN 37996, USA

Submitted by Scott Smith, Oak Ridge National Laboratory, TN, USA

ARTICLE INFO

Article history:
Available online 25 May 2022

Keywords:
Machine tool
Modelling
Monitoring

ABSTRACT

A method is presented to estimate the cutting forces in real time within machine tools for any spindle speed, force profile, tool type, and cutting conditions. Before cutting, a metrology suite and instrumented tool holder are used to induce magnetic forces during spindle rotation, while on-machine vibrations, magnetic forces, and error motions are measured for various combinations of speeds and forces. A physics-inspired data-driven model then relates the measured accelerations to the magnetic forces, such that during cutting, on-machine measured vibrations are used in the model to estimate the cutting forces in real time.

Published by Elsevier Ltd on behalf of CIRP.

1. Introduction

The future of advanced manufacturing depends on transforming traditional machines into “smart” or “intelligent” machine tools with innovative monitoring systems that are robust, reliable, and relatively inexpensive [1,2]. For example, spindles should be integrated with sensors for real-time monitoring of cutting forces and tool-tip displacements so that tool wear and surface quality can be estimated in real time.

However, monitoring cutting forces and tool-tip displacements is difficult because the force measurements require invasive sensors, such as a dynamometer [3], and it is effectively impossible to directly measure the tool-tip displacements during cutting [4]. Dynamometers are the most accurate and reliable force measurement device currently available to industry, but are impractical to use during machining due to workspace constraints and inertial forces that may corrupt the measured forces [5] or reduce the spindle stiffness [2].

Alternatively, indirect methods for estimating cutting forces and tool-tip displacements have been investigated. Cutting force estimation techniques include the use of motor currents [6,7] or spindle-mounted accelerometers [8,9]. Accelerometers are advantageous because they can be mounted within machine tool spindle housings and are robust with relatively high sensitivities and bandwidths [2]. Tool-tip displacements have been estimated in part with measured frequency response functions (FRFs) and receptance coupling substructure analysis (RCSA) [10]. However, FRFs are typically measured without spindle rotation via impact hammer testing, so these static FRF models can be significantly different than the dynamic FRFs, which depend on spindle speed and force levels [11–13]. Such differences can yield inaccurate predictions [11], which implies that the spindle dynamics should be identified under operational conditions with a rotating spindle [12]. Towards this end, various approaches have included the use of a magnetic exciter and capacitive displacement sensors [4], a cutting test procedure [11], and impact testing during rotation with laser vibrometers for radial measurements [13].

Even though considerable research has been conducted to estimate cutting forces and tool-tip displacements with accelerometers and measured FRFs, one main challenge remains: a method must be created to estimate the cutting forces and tool-tip displacements in real-time for any spindle speed, force profile, tool type, and cutting conditions. This paper introduces such a method for force estimation and demonstrates its experimental validation.

2. Method

Fig. 1 shows a high-level overview of the proposed method for real-time estimation of cutting forces using the spindle vibration information measured by accelerometers. This method requires an estimator to relate accelerations to varying forces experienced during machining. The experimental approach was previously reported [14,15] and is summarized here. To generate the estimator, an instrumented tool holder containing a magnet and an embedded laser diode is placed within the machine tool spindle and positioned to interact with a stationary metrology suite located on the machine tool table. During spindle rotation, the rotating magnet of the tool holder interacts with stationary magnets on the metrology suite, generating magnetic forces that simulate cutting forces. The radial separation distance between the stationary and rotating magnets are changed via linear positioning stages to change the radial force profiles. Force profiles in the axial direction can also be changed by modifying the axial position of the tool holder. While other methods have utilized electromagnetic actuation to study spindle dynamics

* Corresponding author.
E-mail address: gvogl@nist.gov (G.W. Vogl).

https://doi.org/10.1016/j.cirp.2022.04.071
0007-8506/Published by Elsevier Ltd on behalf of CIRP.

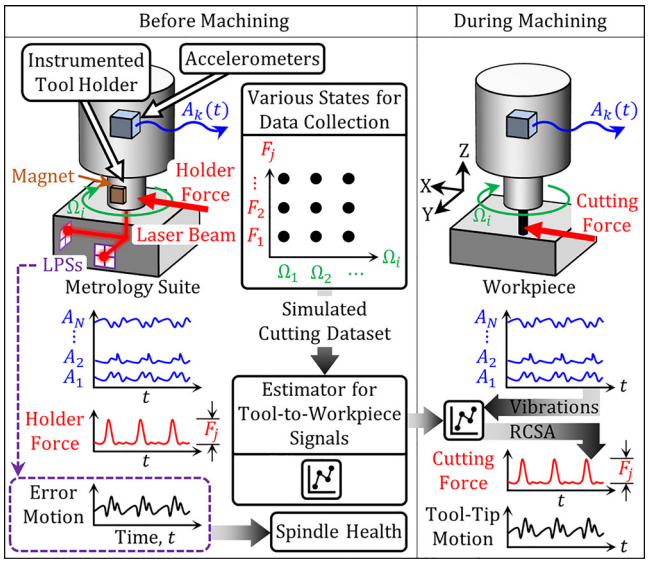

Fig. 1. Schematic of the method for estimating real-time tool-to-workpiece signals (adapted from Refs. [14,15]).

[4,16,17], permanent magnetic forces have advantages such as synchronization to rotation without the need for external triggering and exerting relatively high forces within a reasonable bandwidth. As the tool holder rotates, accelerometers attached to the spindle housing measure the spindle housing vibrations while the forces are measured by commercial strain-gauge-based force-torque sensors. Simultaneously, a laser beam emitted from the laser diode in the tool holder is split into two beams that are detected by laser position sensors (LPSs) in the metrology suite for determination of the spindle radial and tilt error motions. A dataset for simulated cutting conditions is collected for various spindle speeds and force profiles, which is then used to create the estimator relating the spindle vibrations to the forces on the tool holder. Finally, during actual machining, the vibrations are collected and used in the model to estimate the cutting forces in real time. RCSA may also be utilized to improve the force estimates via the inclusion of tool dynamics.

Thus, the method has several advantages over existing methods. The method enables measurements synchronized to rotation without external triggering. Also, no precise alignment is needed between the instrumented tool holder and the metrology suite. Use of an embedded diode laser allows for a relatively short, instrumented tool holder to enable measurements with minimal modal disturbances. Every sensor also has a bandwidth down to 0 Hz, which enables application of the method for low-to-high spindle speeds as well as characterization of the spindle stiffnesses. Furthermore, the method applies to all cutting conditions and tool holders with the same taper mechanism as the instrumented tool holder. Finally, the method does not affect the cutting process and is not affected by workpiece dynamics.

3. Problem formulation and least-squares solution

The estimator relates on-machine vibration displacements, $x_j(t)$, to any force, $F_i(t)$, as a function of spindle speed, Ω, as

$$\mathscr{F}(F_i) = \sum_{j=X,Y,Z} \left[H_{ij}(f).\mathscr{F}(x_j) + \Omega G_{ij}(f).\mathscr{F}(\dot{x}_j) + \Omega^2 N_{ij}(f).\mathscr{F}(x_j) \right] \quad (1)$$

where t is time, f is frequency, $\mathscr{F}$ is the Fourier transform operator, i and j are any of the three axis directions (X, Y, or Z), F_i is the force in the ith direction, x_j is x, y, or z; that is, the measured vibration displacement in the jth direction, an overdot represents differentiation with respect to time, and H_{ij}, G_{ij}, and N_{ij} are FRFs. For any force, Eq. (1) relates that force to all three vibration displacements via nine FRFs. Also, because natural frequencies and damping can change with spindle speed due to gyroscopic moments and centrifugal forces [11–13], the model accounts for these effects with linear and quadratic dependencies on spindle speed [18]. Eq. (1) applies for most cases in which the vibrations are primarily influenced by cutting forces; inertial forces such as those during high-speed contouring are not separated in the method.

The simulated cutting dataset is then used to generate the system of linear equations to solve for the nine FRFs in Eq. (1). First, each data file for a specific spindle speed and force profile is processed with the fast Fourier transform (FFT) to yield the FFTs for Eq. (1). Then, the FFTs are curated to find the frequencies at which at least one of the FFTs has a signal-to-noise amplitude ratio of at least 20. This step excludes the majority of data that is composed of mainly noise and keeps the significant data, at which spindle speed harmonics reside, for modeling purposes. Next, Eq. (1) is applied at each of these significant frequencies, and then the individual frequency components on both sides of the equation are equated to yield a total of M equations that are linear with respect to the nine unknown FRFs. However, the FRFs are functions applied at each of the significant frequencies, and if these unknown function values are treated as independent variables to be solved, then the system of equations would be indeterminate.

To reduce the number of variables and enable a unique solution for the model, every FRF is approximated by linear interpolation between N variables located at the frequencies $f_1, f_2, \ldots, f_N$ with a frequency spacing of Δf, as seen in Fig. 2. This process is similar to that used in another physics-inspired data-driven model [19]. The interpolation of a FRF at a frequency f_m can be expressed with a row vector $\boldsymbol{r}_m = [r_1(f_m), r_2(f_m), \ldots, r_N(f_m)]$ of length N that has elements defined as

$$r_n(f_m) = \begin{cases} (f_{k+1} - f_m)/\Delta f & n = k \\ (f_m - f_k)/\Delta f & n = k+1 \\ 0 & \text{otherwise} \end{cases} \quad (2)$$

where $f_k \leq f_m \leq f_{k+1}$. Consequently, the M equations to model the X-axis force, F_X, may be set up as $\mathbf{A}\boldsymbol{\gamma} = \mathbf{b}$; that is,

$$\mathbf{A} = \begin{bmatrix} \mathscr{F}_1(x)\boldsymbol{r}_1 & \Omega_1.\mathscr{F}_1(\dot{x})\boldsymbol{r}_1 & \Omega_1^2.\mathscr{F}_1(x)\boldsymbol{r}_1 & \cdots \\ \mathscr{F}_2(x)\boldsymbol{r}_2 & \Omega_2.\mathscr{F}_2(\dot{x})\boldsymbol{r}_2 & \Omega_2^2.\mathscr{F}_2(x)\boldsymbol{r}_2 & \\ \vdots & \vdots & \vdots & \cdots \\ \mathscr{F}_M(x)\boldsymbol{r}_M & \Omega_M.\mathscr{F}_M(\dot{x})\boldsymbol{r}_M & \Omega_M^2.\mathscr{F}_M(x)\boldsymbol{r}_M & \end{bmatrix} \quad (3a)$$

$$\boldsymbol{\gamma} = [\boldsymbol{H}_{XX}, \boldsymbol{G}_{XX}, \boldsymbol{N}_{XX}, \boldsymbol{H}_{XY}, \boldsymbol{G}_{XY}, \boldsymbol{N}_{XY}, \boldsymbol{H}_{XZ}, \boldsymbol{G}_{XZ}, \boldsymbol{N}_{XZ}]^T \quad (3b)$$

$$\mathbf{b} = [\mathscr{F}_1(F_X), \mathscr{F}_2(F_X), \ldots, \mathscr{F}_M(F_X)]^T \quad (3c)$$

where $\mathscr{F}_m$ is the component of the FFT at $f = f_m$, Ω_m is the spindle speed for the mth equation, and each of the nine vector components (e.g., $\boldsymbol{H}_{XX}$) within the variable FRF vector $\boldsymbol{\gamma}$ are composed of N unknown FRF values at the frequencies $f_1, f_2, \ldots, f_N$ (see Fig. 2). Note that similar equations may be established to model any force as a function of the vibrations.

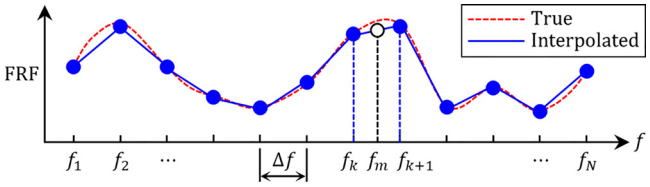

Fig. 2. Illustration of a piecewise linear approximation of a FRF and linear interpolation at a frequency f_m.

Finally, the least-squares solution of the complex matrix equation $\mathbf{A}\boldsymbol{\gamma} = \mathbf{b}$ is $\boldsymbol{\gamma} = (\mathbf{A}^*\mathbf{A})^{-1}\mathbf{A}^*\mathbf{b}$, where $\mathbf{A}^*$ is the conjugate transpose of $\mathbf{A}$. Because the piecewise linear approximations for the nine FRFs ($H_{XX}(f), G_{XX}(f), N_{XX}(f)$, etc.) are known, Eq. (1) estimates $F_X(t)$ given any measured vibrations via the inverse FFT.

4. Experimental setup

To validate the proposed method, it was applied on a vertical machining center, as seen in Fig. 3. First, the metrology suite, instrumented tool holder, accelerometers, and data acquisition (DAQ) box

were set up within the machine tool (see Fig. 3a, b). Each stationary magnet was moved via its linear positioning stage to be as far away from the tool holder as possible. Data was then collected repeatedly at 10 kHz over a duration of 1 s while increasing the spindle speed from 500 rpm to about 7500 rpm with an increment of 37 rpm over a period of about 5 min. Next, the stationary magnet mounted in the X-direction was set closer to the tool holder, such that the force range was about 10 N during rotation. Data was then collected during rotation with the same speed-ramping procedure. Then, the same magnet was repositioned such that the force range was about 20 N, and data was collected again. This process was repeated until the force range was about 80 N. The data collected with various spindle speeds and magnetic forces constitutes the simulated cutting dataset from which the force estimation model will be created. However, due to limitations in generating large forces with the existing setup, the resulting model is most applicable for finish machining operations.

To compare the estimated forces with the actual forces measured during cutting, after the estimator is generated using the simulated

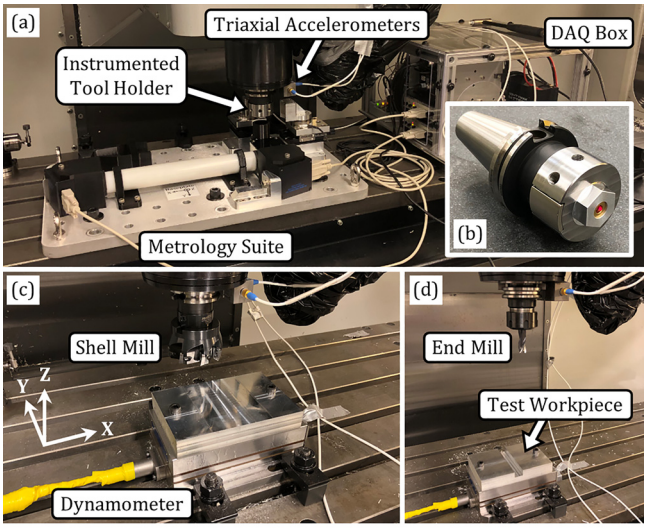

Fig. 3. (a) Metrology suite on machine tool, (b) instrumented tool holder, and (c) shell mill and (d) end mill with dynamometer.

cutting dataset, the instrumentation was removed from the machine tool, but the accelerometers remained on the spindle housing. A dynamometer was then set up on the worktable with an aluminum alloy test workpiece to independently measure cutting forces during machining. Next, cuts were made in the Y-axis direction at a spindle speed of 2500 rpm with an indexable shell mill (see Fig. 3c) having a nominal diameter of 76.2 mm. Six cutting passes were performed with a nominal axial depth of 0.762 mm, radial immersion of 100% (76.2 mm), and feed per tooth from 25.4 µm to 88.9 µm with an increment of 12.7 µm. Finally, a new test workpiece was attached to the dynamometer and cuts were made in the same direction at the same spindle speed of 2500 rpm with a three-fluted end mill (see Fig. 3d) having a nominal diameter of 12.7 mm. Six cutting passes were performed with a nominal axial depth of 6.35 mm, radial immersion of 25% (3.175 mm), and feed per tooth from 25.4 µm to 152.4 µm with an increment of 25.4 µm.

5. Results

An estimator for the X-axis force was created with a frequency spacing Δf of 5 Hz, based on the assumption that modal damping is sufficiently high such that the frequency spacing will capture the frequency changes of the FRFs. A low frequency f_1 (see Fig. 2) was chosen to be 7 Hz, which is less than the lowest speed of 500 rpm. Also, a high frequency f_N of 500 Hz was chosen so that apparent tool-related resonances around 850 Hz, as seen in the measured tool-tip FRFs in Fig. 4, will not affect the force estimation. In this way, RCSA will not be needed for force estimation because each mill is dynamically static for force components below 500 Hz. Furthermore, use of various

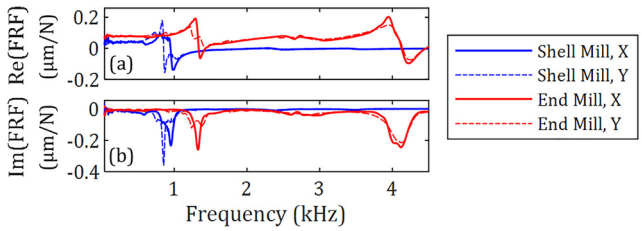

Fig. 4. (a) Real part and (b) imaginary part of the measured tool-tip FRFs for the indexable shell mill and the three-fluted end mill.

subsets of the full dataset revealed that five minutes of collected data per axis is typically needed to achieve a sufficiently accurate force model.

Fig. 5 shows that the proposed method models the dependence of FRFs on spindle speed, in which FRF_{XX}, FRF_{XY}, and FRF_{XZ} are the FRFs relating F_X and the vibrations in the X-, Y-, and Z-direction, respectively. Partial validation is provided via impact testing on the instrumented tool holder with no spindle rotation and 20 impacts for calculations of means and coherences. In general, as seen in Fig. 5, the estimated FRF magnitudes change with spindle speed. Typically, no speed-dependent term in Eq. (1) is dominant except when frequencies are less than 20 Hz, where the centrifugal-related term may dominate. In that regime, as the spindle speed increases, the FRF magnitudes tend to decrease. Thus, vibrations with frequencies less than 20 Hz will decrease for constant force components, possibly due to centrifugal effects.

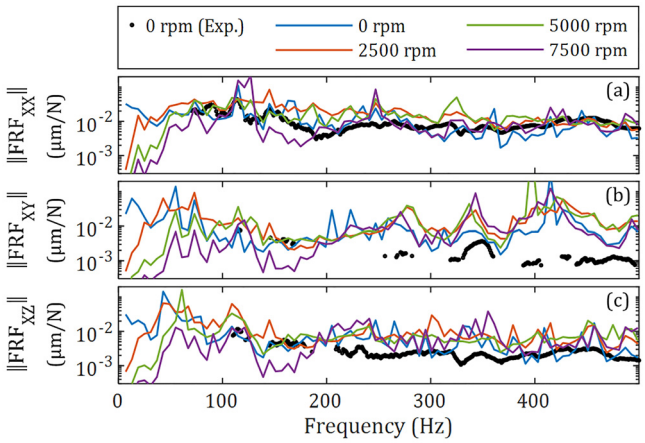

Fig. 5. Magnitudes of (a) X-axis, (b) Y-axis, and (c) Z-axis components of the estimated complex FRF for the X-axis force for various spindle speeds. The experimentally measured values ("Exp.") from impact testing are where coherence ≥ 0.80.

Comparisons of the measured (by dynamometer) and modeled forces are shown in Figs. 6 and 7. The measured forces were low-pass filtered with a cutoff frequency of 500 Hz for a fairer comparison with the modeled forces with the same upper frequency limit. Likewise, the modeled forces were adjusted with direct current (DC)

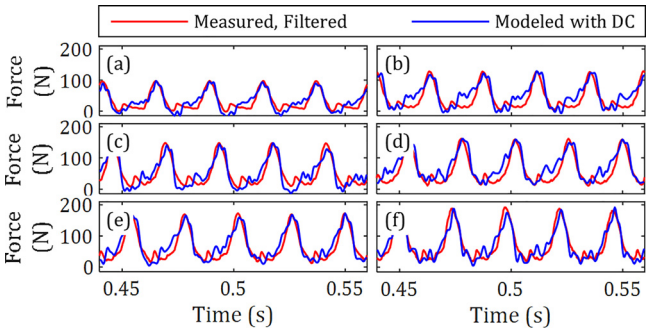

Fig. 6. Measured (by dynamometer) and modeled (with added DC term) X-axis forces for the indexable shell mill with passes of increasing feed per tooth from (a) 25.4 µm (0.001 in) to (f) 88.9 µm (0.0035 in).

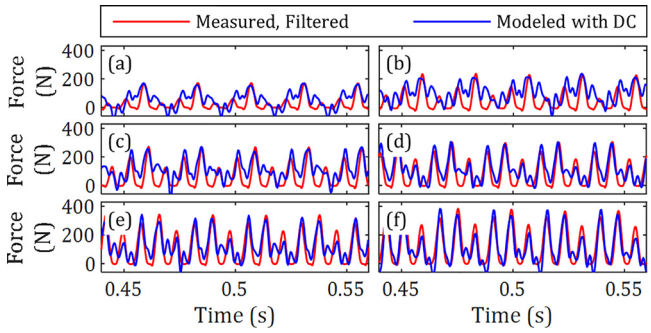

Fig. 7. Measured (by dynamometer) and modeled (with added DC term) X-axis forces for the three-fluted end mill with passes of increasing feed per tooth from (a) 25.4 µm (0.001 in) to (f) 152.4 µm (0.006 in).

terms for matching the peak values of the dynamometer and modeled forces, because the estimator currently does not output DC terms. While DC forces may be theoretically estimated due to sensor bandwidths down to 0 Hz, in practice, the cross-axis sensitivities of the accelerometers corrupted their DC values; reliable estimation of the DC force levels was not achieved. Nonetheless, the range of modeled forces match the range of measured forces fairly well (see Fig. 8), e.g., with a mean absolute error of about four percent for the shell mill test.

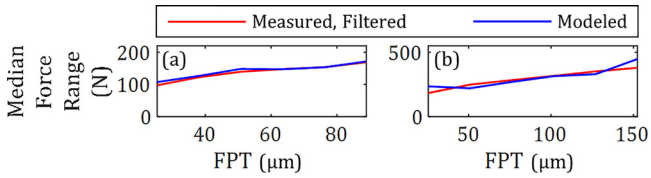

Fig. 8. Median force ranges for the cutting passes for the (a) shell mill and the (b) end mill as a function of feed per tooth (FPT).

6. Conclusions

A new method is proposed to estimate cutting forces in real time during machining via accelerometers and a physics-inspired data-driven model. Before cutting, an instrumented tool holder is rotated to induce magnetic forces measured with a metrology suite while on-machine vibrations are measured with accelerometers. The process simulates cutting for various combinations of spindle speeds and forces. The harmonic content in the simulated cutting dataset is then used to model the speed-dependent relationships between forces and the spindle vibrations. The model is physics-inspired and data-driven because it includes speed dependencies and arises from a least-squares solution instead of physical parameters, respectively. Finally, the model uses the known spindle speed and the accelerations collected during cutting to estimate the cutting forces. Cutting tests and impact testing with two types of milling cutters validated the new approach when tool dynamics can be neglected.

The proposed method was developed for industrial application with any spindle speed, force profile, tool type, and cutting conditions, as well as for potential integration within machine tools to advance the control of milling processes and optimize production. For example, the instrumented tool holder can be installed in a tool-holder carousel, and the metrology suite can be miniaturized for installation and automated usage, similar to tool-setting stations.

Future work includes the advancement of the method via additional sensors, such as motor current sensors, to achieve estimation of DC forces. Another important future task is the extension of the method for modeling radial and tilt error motions. Because the standard deviations of the noise of the radial and tilt error motions are about 0.11 µm and 0.32 µrad, respectively, for a bandwidth of 10 kHz, the error motion changes due to varying forces and spindle speeds are observable. Other future work includes uncertainty analysis of method outputs, testing for all cutting force components on multiple machine tools, optimization of the solution algorithm for real and imaginary terms, the use of RCSA, and modeling with additional nonlinearities.

Declaration of Competing Interest

The authors declare that they have no known competing financial interests or personal relationships that could have appeared to influence the work reported in this paper.

Acknowledgments

The authors thank Dr. Tony Schmitz of the University of Tennessee, Knoxville and the Fabrication Technology Office (NIST) for their outstanding contributions with the experimental setup.

References

[1] Teti R, Jemielniak K, O'Donnell G, Dornfeld D (2010) Advanced Monitoring of Machining Operations. *CIRP Annals-Manufacturing Technology* 59(2):717–739.
[2] Cao HR, Zhang XW, Chen XF (2017) The Concept and Progress of Intelligent Spindles: a Review. *International Journal of Machine Tools & Manufacture* 112:21–52.
[3] Abdullah L, Jamaludin Z, Chiew T, Rafan N (2013) Systematic Method for Cutting Forces Characterization for XY Milling Table Ballscrew Drive System. *Int J Mech Mechatron Eng* 12:28–33.
[4] Kim J, Chang H, Han D, Jang D, Oh S (2005) Cutting Force Estimation by Measuring Spindle Displacement in Milling Process. *CIRP Annals* 54(1):67–70.
[5] Brecher C, Eckel HM, Motschke T, Fey M, Epple A (2019) Estimation of the Virtual Workpiece Quality by the Use of a Spindle-Integrated Process Force Measurement. *CIRP Annals-Manufacturing Technology* 68(1):381–384.
[6] Altintas Y, Aslan D (2017) Integration of Virtual and On-Line Machining Process Control and Monitoring. *CIRP Annals-Manufacturing Technology* 66(1):349–352.
[7] Aslan D, Altintas Y (2018) Prediction of Cutting Forces in Five-Axis Milling Using Feed Drive Current Measurements. *IEEE/ASME Transactions on Mechatronics* 23 (2):833–844.
[8] Postel M, Aslan D, Wegener K, Altintas Y (2019) Monitoring of Vibrations and Cutting Forces with Spindle Mounted Vibration Sensors. *CIRP Annals-Manufacturing Technology* 68(1):413–416.
[9] Wang C, Zhang X, Qiao B, Cao H, Chen X (2019) Dynamic Force Identification in Peripheral Milling Based on CGLS Using Filtered Acceleration Signals and Averaged Transfer Functions. *Journal of Manufacturing Science and Engineering* 141 (6):064501.
[10] Kumar UV, Schmitz TL (2012) Spindle Dynamics Identification for Receptance Coupling Substructure Analysis. *Precision Engineering* 36(3):435–443.
[11] Grossi N, Sallese L, Scippa A, Campatelli G (2017) Improved Experimental-Analytical Approach to Compute Speed-Varying Tool-Tip FRF. *Precision Engineering* 48:114–122.
[12] Yan R, Gao RX, Zhang L (2015) In-Process Modal Parameter Identification for Spindle Health Monitoring. *Mechatronics* 31:42–49.
[13] Bediz B, Gozen BA, Korkmaz E, Ozdoganlar OB (2014) Dynamics of Ultra-High-Speed (UHS) Spindles Used for Micromachining. *International Journal of Machine Tools and Manufacture* 87:27–38.
[14] Qu Y, Vogl GW (2021) Estimating Dynamic Cutting Forces of Machine Tools from Measured Vibrations Using Sparse Regression with Nonlinear Function Basis. In: *Proceedings of the Annual Conference of the PHM Society*, . (Virtual).
[15] Fabro J, Vogl GW, Qu Y (2022) Run-Time Cutting Force Estimation Based on Learned Nonlinear Frequency Response Function. *Journal of Manufacturing Science and Engineering* 144(9). 091002 (11 pages).
[16] Matsubara A, Tsujimoto S, Kono D (2015) Evaluation of Dynamic Stiffness of Machine Tool Spindle by Non-Contact Excitation Tests. *CIRP Annals-Manufacturing Technology* 64(1):365–368.
[17] Stepan G, Beri B, Miklos A, Wohlfart R, Bachrathy D, Porempovics G, et al. (2019) On Stability of Emulated Turning Processes in HIL Environment. *CIRP Annals-Manufacturing Technology* 68(1):405–408.
[18] Gagnol V, Bouzgarrou B, Ray P, Barra C (2007) Model-Based Chatter Stability Prediction for High-Speed Spindles. *International Journal of Machine Tools and Manufacture* 47(7–8):1176–1186.
[19] Vogl GW, Shreve KF, Donmez MA (2021) Influence of Bearing Ball Recirculation on Error Motions of Linear Axes. *CIRP Annals-Manufacturing Technology* 70 (1):345–348.